Origin of Laser-Induced Near-Subwavelength Ripples: Interference between Surface Plasmons and Incident Laser

Min Huang,[†,*] Fuli Zhao,[†] Ya Cheng,[‡] Ningsheng Xu,[†] and Zhizhan Xu[‡,*]

[†]State Key Laboratory of Optoelectronic Materials and Technologies, Sun Yat-sen University, Guangzhou 510275, China, and [‡]State Key Laboratory of High Field Laser Physics, Shanghai Institute of Optics and Fine Mechanics, Chinese Academy of Sciences, P.O. Box 800-211, Shanghai 201800, China

ABSTRACT We show that short-pulse laser-induced classical ripples on dielectrics, semiconductors, and conductors exhibit a prominent "non-classical" characteristic—in normal incidence the periods are definitely smaller than laser wavelengths, which indicates that the simplified scattering model should be revised. Taking into account the surface plasmons (SPs), we consider that the ripples result from the initial direct SP-laser interference and the subsequent grating-assisted SP-laser coupling. With the model, the period-decreasing phenomenon originates in the admixture of the field-distribution effect and the grating-coupling effect. Further, we propose an approach for obtaining the dielectric constant, electron density, and electron collision time of the high-excited surface. With the derived parameters, the numerical simulations are in good agreement with the experimental results. On the other hand, our results confirm that the surface irradiated by short-pulse laser with damage-threshold fluence should behave metallic, no matter for metal, semiconductor, or dielectric, and the short-pulse laser-induced subwavelength structures should be ascribed to a phenomenon of nano-optics.

KEYWORDS: laser-induced near-subwavelength ripples · surface plasmons · SP-laser interference · grating-assisted SP-laser coupling · high-excited surface · nano-optics

Since the early days of the laser, laser-induced damage has been intensively studied for over four decades, not only for its broad industrial applications, but also for the rich physics. Especially in the past decade, the short-pulse laser used in micro/nanomachining, which can offer unique advantages and provide a nanometer-scale precision,[1−3] has given rise to considerable interest. Laser-induced damage is a complex process,[1,4−7] which involves miscellaneous interactions between light and matter, such as laser-induced carrier excitation, carrier thermalization, and various thermal and structural events. In particular, during the irradiation of short-pulse laser, the nonlinear ionization mechanism[1,4−7] plays an important role, and the ablation is achieved *via* an ultrafast, nonthermal process.[8] Thus, experimentally, it is hard to determine the exact physical mechanisms and dynamics occurring in the ablation process *via* certain direct measures or observations of the short-pulse laser-induced high-excited surface. Whereas, *via* certain indirect means, to some extent we can find out in the ultrafast process what has happened. For example, the surface morphological characteristics of the ablated area can provide us significant insights into the understanding of the process. In the paper, *via* the in-depth study of the short-pulse laser-induced surface ripples, we can determine certain dominant mechanisms related to surface plasmons (SPs)[9−16] in short-pulse laser-induced damage. This investigation not only can promote our understanding of laser−solid-matter interaction, but also would contribute to the attractive field of nano-optics[9−15] and the novel concept of ultrafast active plasmonics.[17,18]

In the field of laser-induced damage, laser-induced periodic surface structure is a universal phenomenon, and the classical ripples[19−21] are widely accepted as a result of the interaction between the incident light and the surface scattering wave. Nowadays, the phenomenon has attracted great interest again, because short-pulse laser can easily induce subwavelength ripples.[22−37] In general, the period (Λ) of such ripples may vary in a wide range; according to the ratio (Λ/λ) of Λ to the laser wavelength (λ) in normal incidence, the ripples can be separated into near-subwavelength ripples (NSRs, $0.4 < \Lambda/\lambda < 1$) and deep-subwavelength ripples (DSRs, $\Lambda/\lambda < 0.4$). In respect that the characteristics of DSRs are different greatly from that of the classical ripples,[19−21] it is proposed[23] that DSRs should not be ascribed to the classical ripples described by the scattering

*Address correspondence to syshm@163.com, zzxu@mail.shcnc.ac.cn.

Received for review June 22, 2009 and accepted November 5, 2009.

Published online November 12, 2009.
10.1021/nn900654v

model.[19−21] But until now, the origin of DSRs is still an outstanding issue. On the other hand, the discussion for NSRs has not been paid attention to, for it is always considered as a classical phenomenon, and the picture for such ripples is straightforward: period is expressed as $\Lambda = \lambda/(1 \pm \sin\theta)$ from the simplification of the scattering model; in normal incidence, Λ is considered to be equal to λ. Nevertheless, the model seems to be too simple at present. An increasing number of experimental results show that for short-pulse laser irradiation in normal incident, Λ of such ripples is significantly smaller than λ.[24,32,33,35] Actually, although the simplified scattering model has been widely accepted, it has been suggested that in certain situations,[20,27,31,38,39] such as on metals[20,31] and around specific scattering centers,[38] the scattering model should be revised to take into account the effect of surface electromagnetic wave, that is, SPs. In this paper, with the experimental results on various materials involving dielectrics (ZnO, ZnSe, SiC, and diamond), semiconductors (Si and GaAs), and conductors (graphite and Brass (CuZn)), we demonstrate that for normal incidence, in most of the cases Λ of such ripples is obviously smaller than λ (in general, $0.45 < \Lambda/\lambda < 0.94$). The fact confirms that NSRs also cannot be described by the simplified scattering model. On the basis of the results, we propose that the high-excited characteristic of the surface—laser-induced SPs are responsible for the formation of NSRs, and the model—the initial SP-laser interference and the subsequent grating-assisted SP-laser coupling can provide a complete picture for understanding a variety of phenomena about NSRs.

On the other hand, the laser-induced plasma[26,30,40] and the ionization mechanisms of short-pulse laser in dielectrics[1,4−8] are both active research topics. For the investigations, an important issue is the excited electron density (n_e) for certain critical conditions, such as the damage-threshold n_e. In practice, it is hard to determine n_e accurately at these states, for the situations are always accompanied by phase changes or structural modification, which would hinder the measure. As a result, the damage-threshold n_e can not been quantified by direct experimental methods and commonly is assumed to be the critical density of plasma approximately.[4−7] In addition, currently, because they resemble the surprising optical characteristics of nanostructures on metallic film,[9−15] the optical properties of the nanostructures on the high-excited dielectric surface induced by short-pulse laser have also given rise to great interest.[37] To investigate the optical properties of nanoapertures on such a surface, the dielectric constant (ε) is prerequisite. But similar to n_e, ε for a high-excited surface has also not been achieved by a direct experimental approach. It is well-known that on structured metal SPs are easily launched for abundant free electrons. Actually, for dielectric and semiconductor surfaces, some previous investigations[27,37,38] indicate

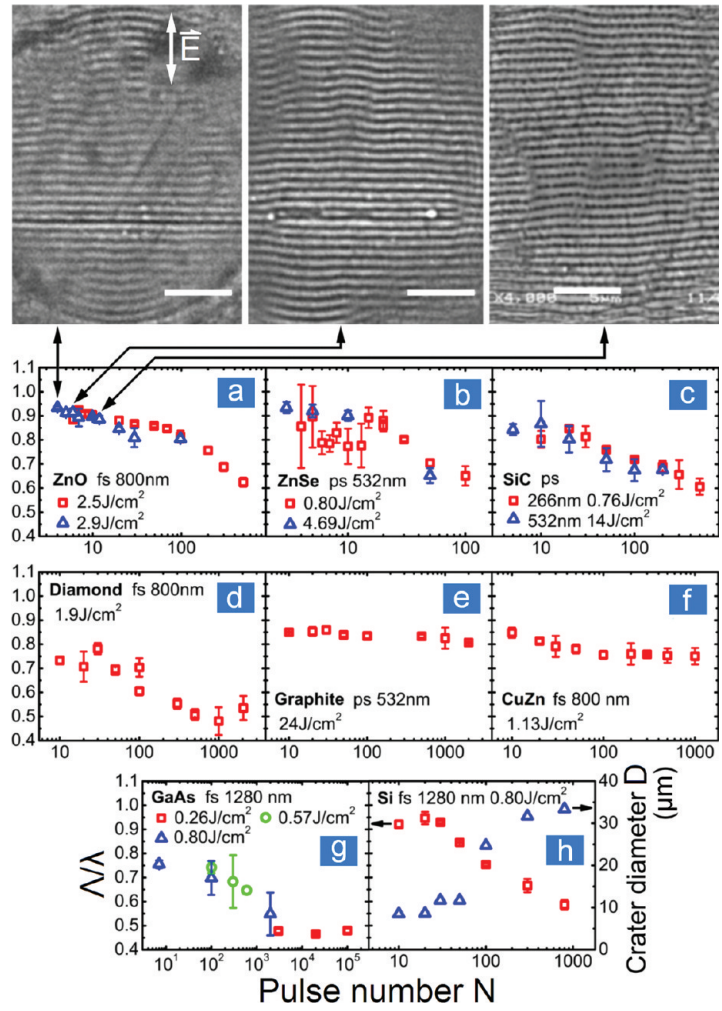

Figure 1. Characteristics of near-wavelength ripples on various materials irradiated by short-pulse laser ablation. Λ/λ as a function of *N* for (a) ZnO, (b) ZnSe, (c) SiC, (d) diamond, (e) graphite, (f) CuZn, (g) GaAs, and (h) Si with irradiation conditions indicated in each figure. In panel h, Λ is measured in the periphery area, and crater diameter *D* as a function of *N* is also exhibited. SEM images for the typical ripples of ZnO irradiated by different pulse numbers are shown (scale bar, 5 μm; double arrow, laser polarization).

that the real part (ε') of ε of a laser-induced high-excited surface may fulfill the metallic condition $\varepsilon' < -1$, therefore such a surface can also support SPs. In the letter, with plenty of substantial experimental results, we further confirm that the damage-threshold surface irradiated by short-pulse laser should exhibit metallic behavior, no matter if it is metal, semiconductor, or dielectric. Furthermore, ε can be obtained from NSRs *via* the SP-laser interference model. Thus, with the Drude model, n_e and the electron collision time (τ_c) can be determined. With the derived parameters, numerical simulations for the high-excited surface have been carried out, and these confirmed the mechanisms for NSRs.

RESULTS AND DISCUSSION

Experimental Results. Figure 1 shows Λ/λ of NSRs as a function of pulse number (*N*) for various materials. In general, when laser fluence and *N* are appropriate, regular NSRs can be observed in the center (small *N*)

or the periphery (large *N*) of the crater with the prominent characteristics—Λ is smaller than λ, and the grating vector of NSRs is definitely parallel to laser polarization (Figure 1a). In addition, as a whole, Λ/λ decreases as *N* is increasing, in agreement with previous reports.[28,32] At large *N*, Λ deviates from λ greatly, and the downward trend is slowing or stops. Interestingly, the Λ-decreasing phenomenon is far more prominent in the cases of dielectrics and semiconductors than the cases of conductors. Moreover, the subwavelength characteristic and the Λ/λ-*N*-decreasing trend of NSRs are not strongly influenced by the laser pulse duration—in the cases of picosecond (ps) and femtosecond (fs) laser ablations, similar characteristics can be observed. But in detail, through the comparison of Figure 1g and Figure 2a for GaAs, we can see that Λ is smaller in the case of fs laser irradiation than in the case of ps laser irradiation. These phenomena are all the common characteristics for NSRs, which will be explained in the discussion part based on our models.

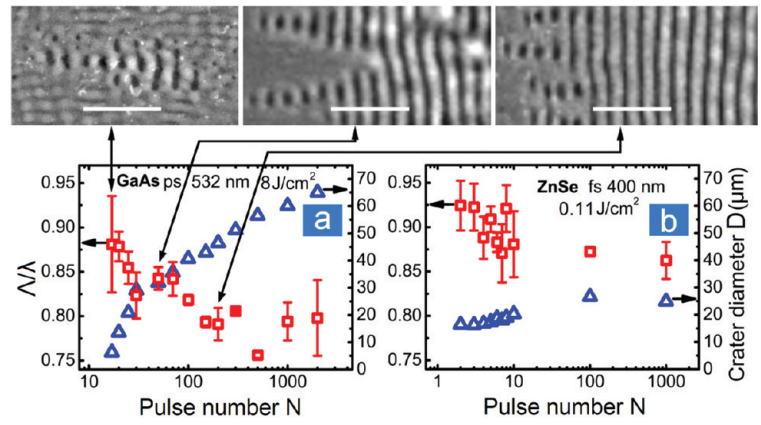

Figure 2. For NSRs of (a) GaAs and (b) ZnSe in the periphery areas of craters, the relationships between Λ/λ and *D* as *N* increases are shown (SEM images demonstrate the ripples of GaAs irradiated with three typical pulse numbers (scale bar, 2 μm)).

Now we focus on the details of certain significant morphological characteristics, which can offer us further insights. First, for NSRs in the periphery area, Λ/λ and crater diameter (*D*) are relevant, as shown in Figure 1h and Figure 2, which indicate that *D* is a factor for Λ decreasing. Second, the large Λ/λ, which always appears at small *N* or in the central area (Figure 3), goes with shallow grooves. In other words, the smooth ripples have large Λ/λ; contrarily, the ripples with deep grooves have small Λ/λ. It means that the groove depth (*H*) is also an important factor for Λ. In addition, NSRs on various materials with different irradiation conditions exhibit more or less the same morphological characteristics, which mean NSRs originate in laser interacting with the high-excited surface, whose optical properties are determined by abundant hot electrons rather than the intrinsic properties.

Discussion. ***Direct SP-Laser Interference.*** As the experimental results shown, NSRs cannot be described by the simplified classical model, which educes that Λ should be equal to λ in normal incidence. Taking into account the crucial phenomenon in strong-field laser−matter interactions−laser-induced plasma, and the well-known laser−plasma interaction in a interface−oscillations of the electron plasma coupled by electromagnetic fields (SPs),[13,16] we consider that the SP-laser interference is responsible for the initialization of NSRs, and the transverse magnetic (TM) characteristic of SPs determines the polarization dependence of ripples. On a metallic surface, SPs can be efficiently launched by subwavelength apertures under laser irradiation.[9−18] For example, the generation of SPs by a single subwavelength slit in a metal screen has been studied theoretically, and under normal incident, the SP-generation efficiency can be fairly large (≈0.5) at visible frequencies.[41,42] Then, the propagating SPs and the incident laser will interfere to form a fringe with a vector (Figure 4a)

$$\mathbf{G} = \mathbf{k}_i - \mathbf{k}_s \qquad (1)$$

where $\mathbf{k}_i$ is the wavevector of incident laser, and $\mathbf{k}_s$ is the wavevector of SPs. Considering the components in the interface, we obtain

$$\Lambda = \frac{\lambda}{\frac{\lambda}{\lambda_s} \pm \sin\theta} \qquad (2)$$

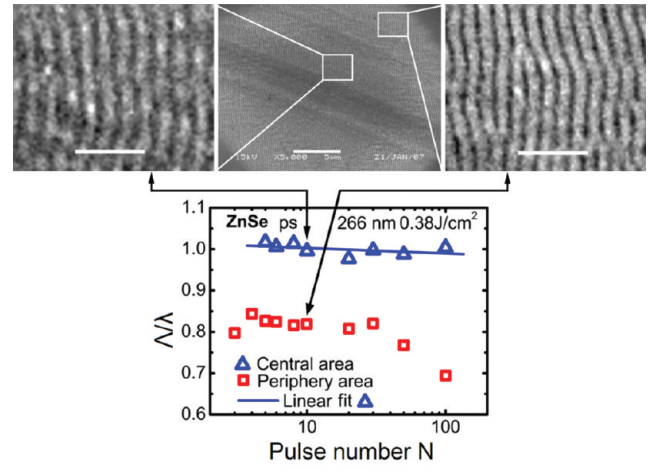

Figure 3. In the case of ZnSe irradiated by short-wavelength pulse, Λ in the central area is different from that in the periphery area, and approximately equal to λ (SEM images demonstrate the ripples in the two areas (scale bar in the enlarged images, 1 μm; scale bar in the overview image, 5 μm)).

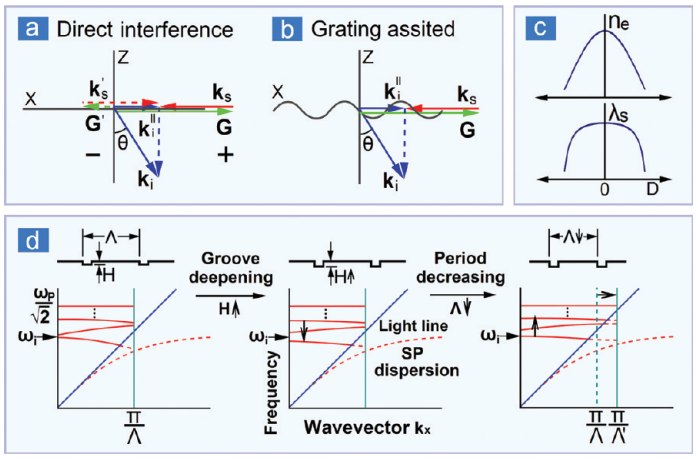

Figure 4. Physical processes involved in the formation of NSRs. Schematic processes of SP-laser interactions: (a) direct SP−laser interference; (b) grating-assisted SP−laser coupling. (c) For the Gaussian distribution of laser fields in the focus, n_e and λ_s both decrease from the center to the periphery of ablated craters. (d) As grooves deepen, the grating-coupling mechanism takes effect and causes Λ to decrease.

where $\Lambda = 2\pi|\mathbf{G}|^{-1}$, $\lambda = 2\pi|\mathbf{k}_i|^{-1}$, $\lambda_s = 2\pi|\mathbf{k}_s|^{-1}$, and θ is the incident angle of laser. Assumed $\varepsilon'' < |\varepsilon'|$ (ε'' is the imaginary part of ε), the λ_s on a metal/dielectric interface is given by[16]

$$\lambda_s = \lambda\left(\frac{\varepsilon' + \varepsilon_d}{\varepsilon'\varepsilon_d}\right)^{1/2} \quad (3)$$

where ε_d is the dielectric constant of the dielectric material (for air, $\varepsilon_d \approx 1$). By eq 2, in normal incidence ($\theta = 0°$) we obtain the simple relationship $\Lambda = \lambda_s$. It means that in the situation with a destructible fluence, the interference fringes will induce permanent ripples on material surface with Λ equal to λ_s, which is always smaller than λ—the characteristic agrees with the experimental observations and is precisely the origin of the subwavelength characteristic of such ripples.

With the $\lambda-\Lambda$ relationship of normal incidence, the $\lambda-\Lambda$ relationship at arbitrary incident angle can be derived by eq 2. As shown in Figure 5, the derived line for 45° agrees with the experimental results, which confirms that eq 2 is a suitable model for NSRs.

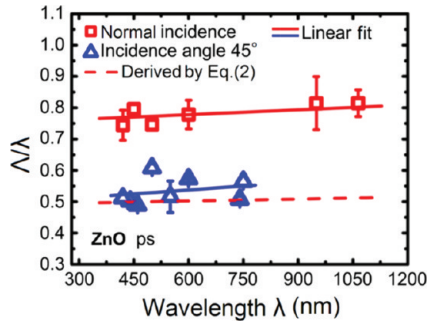

Figure 5. Average Λ/λ as a function of λ for ZnO in normal and tilt (45°) incidents (the dashed line is derived from the normal case by eq 2 (using the plus operation)).

Field-Distribution Effect. Above we have brought forward the essence of the subwavelength characteristic—λ_s is always smaller than λ. Now we give further discussions about the main reasons for the Λ-decreasing phenomenon as N increasing. As described above, Λ in the periphery is related to the crater diameter D. We consider this effect is due to the Gaussian distribution of the fields in the focus. With N increasing, D increases simultaneously, and for such a field distribution, accordingly the fluence in the periphery of the ablated crater is lower and lower. As a result, the periphery n_e decreases as D increases. Owing to the laser-induced plasma, the dielectric constant of the high-excited surface can be described with the Drude model, which is expressed as

$$\varepsilon(\omega) = \varepsilon_c - \frac{\omega_p^2}{\omega(\omega + i\Gamma)} \quad (4)$$

where ε_c is the dielectric constant of material in normal state (without laser-induced free electrons), $\omega_p = (e^2 n_e/(m_{eff}\varepsilon_0))^{1/2}$ is the plasma frequency, and $\Gamma = 1/\tau$ is the electron collision frequency. From eq 4, we obtain $\varepsilon'(\omega) = \varepsilon_c - \omega_p^2/(\omega^2 + \Gamma^2)$. For $\varepsilon' < -1$, with n_e decreasing, $|\varepsilon'|$ decreases, thus from eq 3 λ_s also decreases (Figure 4c), that is, in the periphery Λ gets smaller as D gets larger. This proposal agrees with the observations in Figure 2, which definitely demonstrate that for NSRs in the periphery area Λ gets smaller as D gets larger.

Grating-Assisted SP-Laser Coupling. Note that D increasing is an important, but not the lone reason for Λ decreasing. As shown in the SEM images of Figure 1a, in the central area Λ also decreases as N increases accompanied with groove deepening. This phenomenon is attributed to another important mechanism—grating-assisted SP-laser coupling. When the initial ripples (gratings) are formed, we emphasize that the physical picture should be changed due to the effect of grating-coupling. As long as the phase (momentum) matching condition[9,14,16]

$$m\mathbf{G} = \mathbf{k}_i - \mathbf{k}_s \quad (5)$$

(m is an integer) meets, grating-coupling mechanism will work and influence SP-laser interactions. Actually, since the grating is self-induced by SP-laser interference, here m should be equal to 1. Thus, the phase matching condition reduces to eq 1 if only the interference fringe vector $\mathbf{G}$ is redefined as the grating vector (Figure 4b). The transition from the pure interference mechanism to the grating-coupling mechanism should be a positive feedback process, because it makes laser

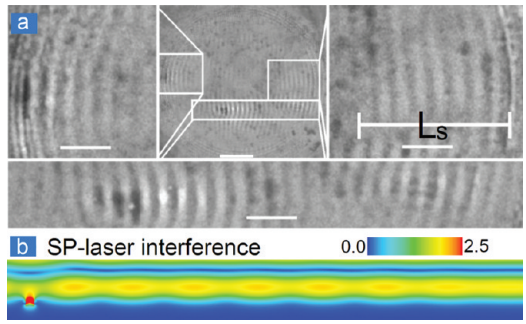

Figure 6. Approach for deriving the parameters of the laser-induced high-excited surface and the simulation result for the picture of direct SP-laser interference. (a) SEM images of a crater on ZnO irradiated by 800-nm fs laser with a fluence of 2.6 J/cm^2 and 5 pulses (scale bar in the enlarged images, 2 μm; scale bar in the overview image, 5 μm). Here Λ and L_s are determined to be 750 and 6000 nm, respectively. (b) With the derived ε, we implement numerical simulations of SP-laser interference launched by a groove (display $|E_x|$ distribution).

fields transfer to SPs more efficiently. Hence grooves will grow as *N* increases and become deeper and deeper. Here we must mention a crucial effect for grating-coupling—as grooves deepen, the resonant wavelength will display a red-shift[10−12,16] (Figure 4d). For grating with deep grooves, in the Brillouin zone the SP dispersion curve is severely modified and tends to be flat, and the group velocity of SP approaches zero; that is, for a specific wavelength, as the groove deepens, Λ should decrease in order to ensure that the grating-coupling condition can be well satisfied, as Figure 4d shows. With this mechanism, we can explain the experimental observations—as *N* increases and grooves deepen, the self-fulfilling of the resonance condition acting as a positive feedback will force Λ to decrease. But there is an exceptional situation. In the crater center, where the fluence is high, the strong thermal effect will induce a thick melted layer (in this case $\varepsilon' \ll -1$ and $\Lambda \approx \lambda$) and baffle the deepening of the groove. Accordingly the grating-coupling effect is weak, and the value of Λ is mainly due to the interference mechanism and remains almost constant near λ as *N* increases (Figure 3). Similarly, we can understand why in long-pulse irradiation Λ is close to λ—the strong thermal effect induces direct interference rather than grating-coupling. In addition, the weak Λ-decreasing phenomenon for conductors can also be attributed to the strong thermal effect as a result of the high heat conductivity of conductors. In contrast, for dielectrics and semiconductors, the nonthermal ablation mechanism makes the deep groove easy to produce, thus the grating-coupling effect is crucial, and the Λ-decreasing phenomenon is prominent.

Derived Parameters and Implement Simulation for High-Excited Surface. From the above discussions, it can be seen that the Λ-decreasing phenomenon is a result of the admixture of the field-distribution effect and the grating-coupling effect, and as long as deep gratings are formed, Λ is no longer approximately equal to λ_s of a flat surface. Therefore, to evaluate the optical (ε) and electronic (n_e) parameters in the high-excited surface through eqs 2−4, we must adopt the data of the initial ripples (small *N*), which exhibit a smooth profile with shallow grooves. From eq 4, ε″ can be expressed as $\varepsilon''(\omega) = \omega_p^2\Gamma/[\omega(\omega^2 + \Gamma^2)]$. Assumed $\varepsilon'' < |\varepsilon'|$, the propagation length of SPs is given by[16]

$$L_s = \frac{\lambda}{2\pi}\left(\frac{\varepsilon' + \varepsilon_d}{\varepsilon'\varepsilon_d}\right)^{3/2}\frac{\varepsilon'^2}{\varepsilon''} \qquad (6)$$

Thus, by measuring the Λ and L_s of localized, shallow ripples launched by a subwavelength aperture, we can obtain ε through solving the equation set including eqs 2 and 6. For instance, such a measurement is performed on ZnO ($\varepsilon_c = 3.85$, $m_{ef} = 0.19m_e$ (m_e is electron mass)) (Figure 6a), and $\Lambda = 750$ nm and $L_s = 6000$ nm are yielded. With the data, $\varepsilon = -8.26 + i1.19$ is derived, and by solving the equation set for ε′ and ε″, $n_e = 4.05 \times 10^{21}$ cm^{-3} and $\tau = 4.31$ fs are obtained. The derived τ is close to the reported value.[40]

With the derived ε, we have carried out numerical simulations for the high-excited surface with the finite difference time domain (FDTD) method.[43,44] Figure 6b shows the SP-laser interference fringe launched by a groove. Obviously, the $|E_x|$ distribution is consistent with the shallow-ripple profile (Figure 6a), and the fringe exhibits Λ equal to λ_s. Further, Figure 7b demonstrates the $|E_x|$ distribution in the case of grating-coupling. As expected, when the grating is formed (grating profile shown in Figure 7a), the grating-coupling disturbs the direct SP-laser interference and makes the field redistribute. The resonant length, Λ, shortens (compare Fig-

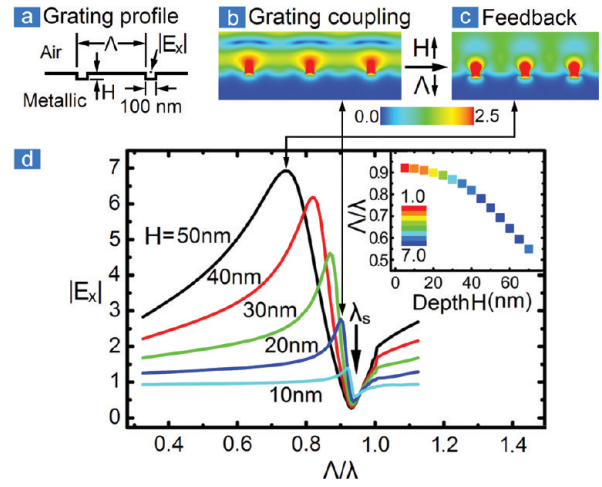

Figure 7. Simulation results for the picture of grating-assisted SP-laser coupling (ε is the same as that in Figure 6): (a) grating profile with the related parameters; $|E_x|$ distribution of grating-assisted SP-laser coupling for (b) shallow grooves (20 nm) and (c) deep grooves (50 nm); (d) for different groove depths, $|E_x|$ in the middle of the groove opening (as the arrow in panel a, indicated) as a function of Λ/λ. Insert is the peaked positions of the curves for different depths (scale bar represents $|E_x|$).

ure 6b with Figure 7b), and the fields in the grooves are extraordinarily enhanced and get stronger as the depth (*H*) increasing (compare Figure 7b with Figure 7c), which implies a strong feedback. As the theory predicted, with *H* increasing, Λ should decrease to ensure the best SP-laser coupling (see the $|E_x|$ distribution from Figure 7b to Figure 7c and Figure 7d—the curves of $|E_x|$ in the middle of the groove opening as a function of Λ/λ for different groove depths). In addition, the curve (inserted in Figure 7d) of the peaked resonant position of Λ as a function of *H* is similar to the trend of the curves of Λ as a function of *N* in Figure 1 and Figure 2, which further confirms the mechanism. On the whole, our simulations agree well with the experimental observations and the theoretical analysis.

Feedback Mechanism of NSRs from the Energy Point of View. As shown by Lalanne *et al.*,[41,42] even for a single subwavelength slit in a metal screen, the SP generation efficiency can achieve 0.5 at visible frequencies. In the case of grating-assisted SP-laser coupling, SPs launched by the periodic grooves fulfilling the phase matching condition can resonate intensively. Such a resonance can boost light scattering into SPs, which is beneficial to the light absorption. It means that the efficiency would be further higher in such a case. As a matter of fact, the metallic subwavelength grating with suitable parameters can almost completely absorb light for a specific wavelength,[45,46] which has given rise to considerable interest in the research fields requiring a high light absorption efficiency, such as the applications in high field laser physics[47,48] and in the field of solar cells.[49,50] As above FDTD simulations demonstrated, along with the grating deepening and the periodicity shortening, light fields are more and more localized in the groove area with field intensity enhanced greatly. Accordingly, it can be expected that as pulse number increases in ablation, the efficiency of grating-assisted SP-laser coupling, that is, the absorption efficiency of the grating surface, should be obviously increased, which leads to the positive feedback of NSRs—the groove deepening and the crater diameter increasing.

To evaluate the light absorption efficiency of NSRs, which can further elaborate the feedback mechanism of NSRs from the energy point of view, we have carried out the calculation of the zeroth-order (specular) reflection efficiency of the grating of Figure 7a with the method of rigorous coupled wave analysis (RCWA).[51,52] The calculation results are shown in Figure 8, which gives the specular reflection efficiency of a vertical incident TM wave as a function of Λ/λ for different groove depths. By comparing Figure 8 with Figure 7d, it can be seen that the dip positions of the reflection efficiency curves are in agreement with the peak positions of the field intensity curves. Resembling the field intensity curves, two prominent characteristics are also exhibited in the reflection efficiency curves: (1) along with the groove depth increasing, the dip position shifts toward

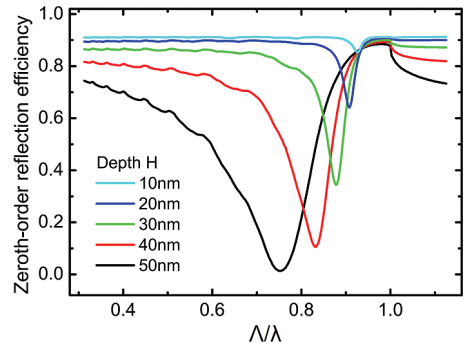

Figure 8. The zeroth-order reflection efficiency of the laser-induced grating as a function of Λ/λ for different groove depths. The grating profile and ε for the reflection calculation is the same as that in Figure 7.

a smaller periodicity; (2) the lowest reflection efficiency decreases strikingly as the groove depth increasing from 10 to 50 nm. For the groove depth of 50 nm, the lowest reflection efficiency can achieve a very low value—about 0.01; that is, the efficiency of grating-assisted SP-laser coupling can achieve near 0.99. It means that in such a case approximately 99%. incident laser energy is absorbed by the grating surface (actually, from the field distributions shown in Figure 7b,c, we can be sure that most of the absorbed energy is localized in the groove area). The results confirm that laser-induced NSRs are able to absorb incident laser energy efficiently, which in turn promotes the formation of NSRs and accelerates the laser ablation process. Recently, the phenomena of enhanced absorption of metal surfaces structured by ultrafast laser irradiation (called "black metal") have attracted people's attention.[53−55] The experimental results[53,54] show that with an increase in the pulse number, the absorptance of the structured surface increases markedly. As our calculation shown, the high light absorption efficiency of the laser-induced NSRs should play an important role for the phenomenon. Conversely, as an inverse process, NSRs may help to the luminous efficiency of light-emitting materials. Nowadays, the phenomenon of a significant increase in the emission efficiency of incandescent light sources treated by femtosecond laser has been observed.[56] In our opinion, the laser-induced NSRs may contribute greatly to the enhancement of the emission efficiency of tungsten lamp *via* the inverse grating-assisted SP-light coupling: the trend that emittance (absorbance) is enhanced following the increase of pulse number is mainly attributed to the growth of laser-induced NSRs, which can improve the efficiency of grating-assisted SP-light coupling; the partially polarized characteristic of the emission light should ascribe to the TM characteristic of grating-assisted SP-light coupling. On the whole, our propositions in the paper can provide specific explanations for the related phenomena.

CONCLUSIONS

The short-pulse laser ablation experiments on various materials indicate that NSRs are always produced, which strongly suggests that the simplified scattering model should be modified to take into account the effect of SPs. In detail, we consider that in the initial stage of NSR formation, the SP-laser interference is the dominant mechanism, and as ripples grow, the grating-assisted SP-laser coupling plays the most important role. With the model, the period-decreasing phenomenon originates in the admixture of the field-distribution effect and the grating-coupling effect. Furthermore, we propose an approach for obtaining the dielectric constant, the electron density, and the electron collision time of the high excited surface *via* NSRs. This approach is significant for the investigation of the ionization mechanisms of short-pulse laser. With the derived parameters, the numerical simulations are consistent with the experimental results, and confirm our propositions about the mechanisms for NSRs. In addition, our results indicate that for the laser-induced ripples, the simplified classical model is only a particular instance of eq 2, which occurs easily in the cases of long-pulse laser or short wavelength laser irradiation, where λ_s is near λ, or the SP effect can be ignored. Although DSRs have not been touched on here, we hold that the propositions for NSRs are of great help for understanding DSRs, which are due to the standing SP wave[37] and the grating-coupling model with a period equal to or smaller than $\lambda_s/2$. In short, this study can provide the exact physical mechanisms for NSRs and significant insights into DSRs, and greatly promote our understanding of the interaction between short-pulse laser and solid materials.

On the other hand, our results confirm that the surface irradiated by short-pulse laser with damage-threshold fluence should exhibit metallic behavior, no matter if it is metal, semiconductor, or dielectric, and in the process of laser-induced optical breakdown, the oscillations of the electron plasma coupled by electromagnetic fields play a crucial role. Especially for the periodic subwavelength apertures, the extraordinary enhancement of fields can occur *via* the self-fulfilling certain SP modes, and *via* a positive feedback process, periodic subwavelength patterns will appear on the surface of material. As a matter of fact, these short-pulse laser-induced subwavelength structures should be ascribed to a phenomenon of nano-optics. To investigate the phenomena of short-pulse laser-induced damage, we should base our work on the microscopic rather than the macroscopic point of view, that is, we should focus on the nano-optics effect of the subwavelength apertures, instead of handling the irradiated area as a perfect surface or bulk without any defect or nanoaperture and considering only the processes of electron excitation and thermalization without the feedback of nano-optics effect. To our knowledge, the field of nano-optics always focuses on metallic materials, where SPs can be easily excited and induce surprising optical properties that have great potential in nanophotonic devices. Our results confirm that the nano-optics mechanisms for metallic materials are also applicable to the field of strong-field laser−solid-matter interaction, that is, our research will extend the scope of nano-optics to the domain of strong-field. In addition, our results indicate that under high-fluence short-pulse laser irradiation, in an ultrashort time scale, the dielectric constant of material can be tuned from being dielectric to metallic, and the plasmonic effect will be activated. This phenomenon could enrich the approaches for realizing the ultrafast active plasmonics.

METHODS

Materials. For the ablation experiments of dielectrics, optical polishing ZnO, ZnSe, and SiC crystals with dimensions of $10 \times 10 \times 1$ mm^3, as well as a natural single-crystal bulk diamond with optical polishing, were used as the samples. For the ablation experiments of semiconductors, optical polishing Si, GaAs single-chips were used. For the ablation experiments of conductors, brass (CuZn) and highly oriented pyrolytic graphite (*c*-axis oriented along the normal of the flake) sheets were used.

Laser Ablation Experiments. A regenerative Ti:Sapphire oscillator−amplifier system (Spectra Physics Hurricane), which ran at a central wavelength of 800 nm with a pulse duration of 125 fs and a repetition rate of 1 kHz, was used to perform femtosecond (fs) ablation experiments. The picosecond (ps) pulses of different wavelengths were obtained by the optical parametric generators (OPGs, EKSPLA, PG411/511) pumped with a mode locked Nd:YAG laser (EKSPLA, PL2143B), which had a pulse duration of 30 ps and a repetition rate of 10 Hz. A variable neutral density filter was used to adjust the pulse energy. Then the linearly polarized Gaussian laser beam was focused on the sample surface by a convex lens (Newport, UV Fused Silica Precision Plano-Convex Lens, focal length 300 mm), and the number of laser pulses imposed per site was determined by an electric shutter. The samples were mounted on an electric XYZ-translation stage, and observed real-time by a CCD monitor equipped with an objective lens of long focus. All experiments were performed in ambient air. The morphologies of ablated spots were observed by scanning electron microscopy (SEM, JEOL JSM-6380 and Quanta 400F).

Numerical Simulations. The numerical simulations of the field distribution on the rippled surface irradiated by fs laser were implemented by the FDTD method[43,44] with an 800-nm TM wave of vertical incidence. The simulation parameters were derived from the initial localized NSRs *via* the SP-laser interference model and the Drude model for the dielectric constant. The method is described in detail in the discussion part.

In addition, the reflective properties of NSRs are analyzed numerically using RCWA method[51,52] with an 800-nm TM wave of vertical incidence. The modeled structure and the dielectric constant for the reflection calculation are the same as that for the FDTD simulation. For a subwavelength metallic grating, that is, a zeroth-order metallic grating, only the zeroth reflected order (the specular reflectivity) can reflect from the grating, and the other orders are evanescent. When there exists a high efficiency of grating-assisted SP-laser coupling, the incident laser light will mostly convert to SPs, which eventually dissipate as heat, and as a result present a low specular reflectivity. Therefore, *via* the cal-

culation of the specular reflectivity of such a grating, we can quantitatively evaluate the efficiency of grating-assisted SP-laser coupling.

Acknowledgment. The authors are grateful to Y. F. Liu and X. R. Zeng for their support in the experiments. This work has been supported by grants from the Shanghai Institute of Optics and Fine Mechanics (SIOM), Chinese Academy of Sciences (CAS).

REFERENCES AND NOTES

1. Gattass, R. R.; Mazur, E. Femtosecond Laser Micromachining in Transparent Materials. *Nat. Photon.* **2008**, *2*, 219–225.
2. Pronko, P. P.; Dutta, S. K.; Squier, J.; Rudd, J. V.; Du, D.; Mourou, G. Machining of Sub-Micron Holes Using a Femtosecond Laser at 800 nm. *Opt. Commun.* **1995**, *114*, 106–110.
3. Chichkov, B. N.; Momma, C.; Nolte, S.; von Alvensleben, F.; Tünnermann, A. Femtosecond, Picosecond and Nanosecond Laser Ablation of Solids. *Appl. Phys. A: Mater. Sci. Process.* **1996**, *63*, 109–115.
4. Stuart, B. C.; Feit, M. D.; Rubenchik, A. M.; Shore, B. W.; Perry, M. D. Laser-Induced Damage.in Dielectrics with Nanosecond to Subpicosecond. Pulses. *Phys. Rev. Lett.* **1995**, *74*, 2248–2251.
5. Tien, A.-C.; Backus, S.; Kapteyn, H.; Mumane, M.; Mourou, G. Short-Pulse Laser Damage in Transparent Materials as a Function of Pulse Duration. *Phys. Rev. Lett.* **1999**, *82*, 3883–3886.
6. Schaffer, C. B.; Brodeur, A.; Mazur, E. Laser-Induced Breakdown and Damage in Bulk Transparent Materials Induced by Tightly Focused Femtosecond Laser Pulses. *Meas. Sci. Technol.* **2001**, *12*, 1784–1794.
7. Sudrie, L.; Couairon, A.; Franco, M.; Lamouroux, B.; Prade, B.; Tzortzakis, S.; Mysyrowicz, A. Femtosecond Laser-Induced Damage and Filamentary Propagation in Fused Silica. *Phys. Rev. Lett.* **2002**, *89*, 186601.
8. Stoian, R.; Rosenfeld, A.; Ashkenasi, D.; Hertel, I. V.; Bulgakova, N. M.; Campbell, E. E. B. Surface Charging and Impulsive Ion Ejection during Ultrashort Pulsed Laser Ablation. *Phys. Rev. Lett.* **2002**, *88*, 097603.
9. Ebbesen, T. W.; Lezec, H. J.; Ghaemi, H. F.; Thio, T.; Wolff, P. Extraordinary Optical Transmission through Sub-Wavelength Hole Arrays. *Nature* **1998**, *391*, 667–669.
10. López-Rios, T.; Mendoza, D.; García-Vidal, F. J.; Sánchez-Dehesa, J.; Pannetier, B. Surface Shape Resonances in Lamellar Metallic Gratings. *Phys. Rev. Lett.* **1998**, *81*, 665–668.
11. Porto, J. A.; García-Vidal, F. J.; Pendry, J. B. Transmission Resonances on Metallic Gratings with Very Narrow Slits. *Phys. Rev. Lett.* **1999**, *83*, 2845–2848.
12. García-Vidal, F. J.; Lezec, H. J.; Ebbesen, T. W.; Martín-Moreno, L. Multiple Paths to Enhance Optical Transmission through a Single Subwavelength Slit. *Phys. Rev. Lett.* **2003**, *90*, 213901.
13. Barnes, W. L.; Dereux, A.; Ebbesen, T. W. Surface Plasmon Subwavelength Optics. *Nature* **2003**, *424*, 824–830.
14. Genet, C.; Ebbesen, T. W. Light in Tiny Holes. *Nature* **2007**, *445*, 39–46.
15. Liu, H.; Lalanne, P. Microscopic Theory of the Extraordinary Optical Transmission. *Nature* **2008**, *452*, 728–731.
16. Raether, H. *Surface Plasmons on Smooth and Rough Surfaces and on Gratings*; Springer-Verlag: Berlin, 1988.
17. Krasavin, A. V.; Zheludev, N. I. Active Plasmonics: Controlling Signals in Au/Ga Waveguide Using Nanoscale Structural Transformations. *Appl. Phys. Lett.* **2004**, *84*, 1416–1418.
18. MacDonald, K. F.; Sámson, Z. L.; Stockman, M. I.; Zheludev, N. I. Ultrafast Active Plasmonics. *Nat. Photon.* **2009**, *3*, 55–58.
19. Emmony, D. C.; Howson, R. P.; Willis, L. J. Laser Mirror Damage in Germanium at 10.6 μm. *Appl. Phys. Lett.* **1973**, *23*, 598–600.
20. Sipe, J. E.; Young, J. F.; Preston, J. S.; van Driel, H. M. Laser-Induced Periodic Surface Structure, I. Theory. *Phys. Rev. B* **1983**, *27*, 1141–1154.
21. Young, J. F.; Preston, J. S.; van Driel, H. M.; Sipe, J. E. Laser-Induced Periodic Surface Structure, II. Experiments on Ge, Si, Al, and Brass. *Phys. Rev. B* **1983**, *27*, 1155–1172.
22. Ozkan, A. M.; Malshe, A. P.; Railkar, T. A.; Brown, W. D.; Shirk, M. D.; Molian, P. A. Femtosecond Laser-Induced Periodic Structure Writing on Diamond Crystals and Microclusters. *Appl. Phys. Lett.* **1999**, *75*, 3716–3718.
23. Reif, J.; Costache, F.; Henyk, M.; Pandelov, S. V. Ripples Revisited: Nonclassical Morphology at the Bottom of Femtosecond Laser Ablation Craters in Transparent Dielectrics. *Appl. Surf. Sci.* **2002**, *197*−*198*, 891–895.
24. Borowiec, A.; Haugen, H. K. Subwavelength Ripple Formation on the Surfaces of Compound Semiconductors Irradiated with Femtosecond Laser Pulses. *Appl. Phys. Lett.* **2003**, *82*, 4462–4464.
25. Wu, Q.; Ma, Y.; Fang, R.; Liao, Y.; Yu, Q.; Chen, X.; Wang, K. Femtosecond Laser-Induced Periodic Surface Structure on Diamond Film. *Appl. Phys. Lett.* **2003**, *82*, 1703–1705.
26. Shimotsuma, Y.; Kazansky, P. G.; Qiu, J.; Hirao, K. Self-Organized Nanogratings in Glass Irradiated by Ultrashort Light Pulses. *Phys. Rev. Lett.* **2003**, *91*, 247405.
27. Pedraza, A. J.; Guan, Y. F.; Fowlkes, J. D.; Smith, D. A. Nanostructures Produced by Ultraviolet Laser Irradiation of Silicon. I. Rippled Structures. *J. Vac. Sci. Technol. B* **2004**, *22*, 2823–2835.
28. Bonse, J.; Munz, M.; Sturm, H. Structure Formation on the Surface of Indium Phosphide Irradiated by Femtosecond Laser Pulses. *J. Appl. Phys.* **2005**, *97*, 013538.
29. Jia, T. Q.; Chen, H. X.; Huang, M.; Zhao, F. L.; Qiu, J. R.; Li, R. X.; Xu, Z. Z.; He, X. K.; Zhang, J.; Kuroda, H. Formation of Nanogratings on the Surface of a ZnSe Crystal Irradiated by Femtosecond Laser Pulses. *Phys. Rev. B* **2005**, *72*, 125429.
30. Bhardwaj, V. R.; Simova, E.; Rajeev, P. P.; Hnatovsky, C.; Taylor, R. S.; Rayner, D. M.; Corkum, P. B. Optically Produced Arrays of Planar Nanostructures Inside Fused Silica. *Phys. Rev. Lett.* **2006**, *96*, 057404.
31. Wang, J.; Guo, C. Formation of Extraordinarily Uniform Periodic Structures on Metals Induced by Femtosecond Laser Pulses. *J. Appl. Phys.* **2006**, *100*, 023511.
32. Hsu, E. M.; Crawford, T. H. R.; Tiedje, H. F.; Haugen, H. K. Periodic Surface Structures on Gallium Phosphide after Irradiation with 150 fs-7 ns laser pulses at 800 nm. *Appl. Phys. Lett.* **2007**, *91*, 111102.
33. Tomita, T.; Kinoshita, K.; Matsuo, S.; Hashimoto, S. Effect of Surface Roughening on Femtosecond Laser-Induced Ripple Structures. *Appl. Phys. Lett.* **2007**, *90*, 153115.
34. Huang, M.; Zhao, F. L.; Cheng, Y.; Xu, N. S.; Xu, Z. Z. Large Area Uniform Nanostructures Fabricated by Direct Femtosecond Laser Ablation. *Opt. Express* **2008**, *16*, 19354–19365.
35. Tomita, T.; Fukumori, Y.; Kinoshita, K.; Matsuo, S.; Hashimoto, S. Observation of Laser-Induced Surface Waves on Flat Silicon Surface. *Appl. Phys. Lett.* **2008**, *92*, 013104.
36. Luo, C. W.; Lee, C. C.; Li, C. H.; Shih, H. C.; Chen, Y.-J.; Hsieh, C. C.; Su, C. H.; Tzeng, W. Y.; Wu, K. H.; Juang, J. Y.; *et al.* Ordered YBCO sub-micron array structures induced by pulsed femtosecond laser irradiation. *Opt. Express* **2008**, *16*, 20610–20616.
37. Huang, M.; Zhao, F. L.; Cheng, Y.; Xu, N. S.; Xu, Z. Z. Mechanisms of Ultrafast Laser-Induced Deep-Subwavelength Gratings on Graphite and Diamond. *Phys. Rev. B* **2009**, *79*, 125436.
38. Keilmann, F.; Bai, Y. H. Periodic Surface Structures Frozen into CO_2 Laser-Melted Quartz. *Appl. Phys. A: Mater. Sci. Process.* **1982**, *29*, 9–18.
39. Brueck, S. R. J.; Ehrlich, D. J. Stimulated Surface−Plasma−Wave Scattering and Growth of a Periodic Structure in Laser-Photodeposited Metal Films. *Phys. Rev. Lett.* **1982**, *48*, 1678–1681.

40. Sun, Q.; Jiang, H.; Liu, Y.; Wu, Z.; Yang, H.; Gong, Q. Measurement of the Collision Time of Dense Electronic Plasma Induced by a Femtosecond Laser in Fused Silica. *Opt. Lett.* **2005**, *30*, 320–322.
41. Lalanne, P.; Hugonin, J. P.; Rodier, J. C. Theory of Surface Plasmon Generation at Nanoslit Apertures. *Phys. Rev. Lett.* **2005**, *95*, 263902.
42. Lalanne, P.; Hugonin, J. P.; Rodier, J. C. Approximate Model for Surface-Plasmon Generation at Slit Apertures. *J. Opt. Soc. Am. A* **2006**, *23*, 1608–1615.
43. EM Explorer, http://www.emexplorer.net. (Accessed 2007.)
44. Taflove, A.; Hagness, S. C. *Computational Electrodynamics: The Finite-Difference Time-Domain Method*, 2nd ed.; Artech House: Norwood, MA, 2000.
45. Loewen, E. G.; Popov E. *Diffraction Gratings and Applications*; Marcel Dekker: New York, 1997; p 298.
46. Popov, E.; Maystre, D.; McPhedran, R. C.; Nevière, M.; Hutley, M. C.; Derrick, G. H. Total Absorption of Unpolarized Light by Crossed Gratings. *Opt. Express* **2008**, *16*, 6146–6155.
47. Murnane, M. M.; Kapteyn, H. C.; Gordon, S. P.; Bokor, J.; Glytsis, E. N.; Falcone, R. W. Efficient Coupling of High-Intensity Subpicosecond Laser Pulses into Solids. *Appl. Phys. Lett.* **1993**, *62*, 1068–1070.
48. Subhendu, Kahaly; Yadav, S. K.; Wang, W. M.; Sengupta, S.; Sheng, Z. M.; Das, A.; Kaw, P. K.; Ravindra Kumar, G. Near-Complete Absorption of Intense, Ultrashort Laser Light by Sub-λ Gratings. *Phys. Rev. Lett.* **2008**, *101*, 145001.
49. Claus, H.; Rudolf, H. M. Submicrometer Gratings for Solar Energy Applications. *Appl. Opt.* **1995**, *34*, 2476–2482.
50. Bermel, P.; Luo, C.; Zeng, L.; Kimerling, L. C.; Joannopoulos, J. D. Improving Thin-Film Crystalline Silicon Solar Cell Efficiencies with Photonic Crystals. *Opt. Express* **2007**, *15*, 16986–17000.
51. Moharam, M. G.; Gaylord, T. K. Rigorous Coupled-Wave Analysis of Planar-Grating Diffraction. *J. Opt. Soc. Am.* **1981**, *71*, 811–818.
52. *RODIS Software Package*; Photonics Research Group: University of Ghent, Belgium. http://www.photonics.intec.ugent.be/research/facilities/design/rodis/default.htm. (Accessed 2009.)
53. Vorobyev, A. V.; Guo, C. Enhanced Absorptance of Gold Following Multipulse Femtosecond Laser Ablation. *Phys. Rev. B* **2005**, *72*, 195422.
54. Vorobyev, A. V.; Guo, C. Effects of Nanostructure-Covered Femtosecond Laser-Induced Periodic Surface Structures on Optical Absorptance of Metals. *Appl. Phys. A: Mater. Sci. Process.* **2007**, *86*, 321–324.
55. Yang, Y.; Yang, J.; Liang, C.; Wang, H. Ultra-Broad Band Enhanced Absorption of Metal Surfaces Structured by Femtosecond Laser Pulses. *Opt. Express* **2008**, *16*, 11259–11265.
56. Vorobyev, A. V.; Guo, C. Brighter Light Sources from Black Metal: Significant Increase in Emission Efficiency of Incandescent Light Sources. *Phys. Rev. Lett.* **2009**, *102*, 234301.